

Measurement-induced Clock in a Lattice Ring of Non-interacting Electrons

David S. Schlegel^{1,2,*} and Stefan Kehrein^{3,†}

¹Laboratory of Theoretical Physics of Nanosystems (LTPN), Institute of Physics, École Polytechnique Fédérale de Lausanne (EPFL), CH-1015 Lausanne, Switzerland

²Center for Quantum Science and Engineering, École Polytechnique Fédérale de Lausanne (EPFL), CH-1015 Lausanne, Switzerland

³Institute for Theoretical Physics, Georg-August-Universität Göttingen, Friedrich-Hund-Platz 1, 37077 Göttingen, Germany

(Dated: January 1, 2024)

We examine the emergence of periodicity in a non-interacting steady-state quantum system without external drive inspired by quantum time crystals' spontaneous time-translation symmetry breaking. Specifically, we consider a lattice ring of non-interacting electrons undergoing weak local position measurements. Our analysis uncovers time-periodic structures in steady-state two-time correlation functions, with periodicity linked to the system's group velocity. This study demonstrates a measurement-induced clock mechanism, highlighting periodic behaviors in two-time correlators of a non-equilibrium steady state, contributing to understanding time-periodic phenomena in minimally interactive quantum systems.

I. INTRODUCTION

Open quantum systems, which explicitly consider the interaction between the system and its environment, have become a major field of study [1–3], shedding light on fundamental processes such as dephasing, decoherence, and particle loss [3–7]. They play a pivotal role in understanding a wide range of experimental setups in quantum science and technology, such as photonic systems [8–11], ultracold atoms [12–16], condensed matter systems [1, 17–22], and chemical physics [23, 24]. Additionally, they are particularly crucial in quantum computation, where quantum bits are sensitive to decoherence due to environmental interaction [25]. Open quantum systems also display emergent phenomena, in particular, dissipative phase transitions [20, 26–30] and topological phases [31–35].

Spontaneous symmetry breaking is a ubiquitous phenomenon observed in nature, underpinning a diverse array of phenomena. This phenomenon is characterized by a situation in which the equations that govern a system exhibit a certain degree of symmetry, but the system selects a solution in a spontaneous manner that breaks this symmetry. This effect can be attributed to the susceptibility of exact symmetric eigenstates to infinitesimally weak perturbations. In particular, the spontaneous breaking of time-translation symmetry, in which a quantum many-body system self-organizes in time and starts spontaneously to undergo a periodic motion, is a key characteristic of quantum *time crystals* [36], opening up new avenues for exploring non-equilibrium phases of matter in interacting quantum systems.

Although it has been proven that time-translation symmetry cannot spontaneously be broken in the ground

state of quantum-systems [37, 38], the formation of *discrete* time-crystals in driven out-of-equilibrium systems can be studied theoretically in the framework of *Floquet theory* [29, 39–44]. Recently, discrete time crystals have also been observed experimentally [45–51]. In these systems, many-body interactions play a fundamental role in the formation of periodic motion with a period different from the external drive [40, 42, 44, 46, 52, 53]. Tremendous efforts have been made to understand time crystallinity in open quantum systems [54–58], where no-go theorems for time crystals in the ground state of closed systems do not apply [41].

In recent studies, repeatedly measuring a quantum system revealed various measurement-induced phenomena, such as measurement-induced quantum jumps [59], measurement-induced nonlocality [60–63], and measurement-induced phase transitions [64–70] in particular.

In many theoretical studies of time crystals and systems of measurement-induced phenomena, many-body interactions play a fundamental role. An interesting and less explored question is whether, instead of many-body interactions, time-periodicity can be observed in non-interacting but solely dissipative systems in their steady state, without the need for external drives or many-body interactions, in which only the interaction with the environment in the form of continuous measurements induces periodic motion in the system.

In this work, we answer this question in the affirmative by realizing a *measurement-induced clock* in an open quantum system out of equilibrium. We propose a toy model consisting of a ring of non-interacting electrons on a lattice, described by a tight-binding model. The system is subject to local dissipators, resembling continuous local position measurements.

We analyze the system's dynamics using two approaches: the Lindblad master equation and the quantum trajectory method. We exactly solve the system for uniform dissipation at every lattice site. We observe long-

* david.schlegel@epfl.ch

† stefan.kehrein@theorie.physik.uni-goettingen.de

lived decaying oscillations in two-time correlators with a bimodal probability current distribution in the steady state. Throughout the dynamics, the repeated measurements localize the wave function of individual quantum trajectories in space so that the system remains highly localized throughout its dynamics, reminiscent of soliton dynamics [71]. As a change of direction of the system's wave function occurs at a characteristic time scale, the two-time correlations in the steady-state ultimately fade. The toy model of a measurement-induced clock explored in this work shows rich dynamical behavior in the absence of many-body interactions and solely induced by measurements from an environment.

We describe the system setup in Sec. II and detail our results in Sec. III. Sec. IV contains the conclusions and outlook.

II. SYSTEM SETUP

Hereinafter, we will analyze a tight-binding model for non-interacting electrons on a lattice with periodic boundary conditions that couple to an environment acting locally on the system, as sketched in Fig. 1(a). With this model, we investigate temporal structures with a particular focus on the steady state. In order to closely resemble the situation of an experimental setup, we model the system's environment by dissipators that depend on the position of the lattice. This can be viewed as continuously probing the system by a measurement apparatus that acts locally on the system and thereby induces dissipation. Such a position-dependent coupling to an environment can generally be described using an effective Lindblad master equation with quasi-local Lindblad operators, describing the reduced system dynamics, as long as the environmental interaction allows for a Markovian approximation.

As the environment is exciting the system, we would intuitively expect the particle to gain momentum, starting from the ground state. The quasi-local Lindblad operators of the dissipation mechanism would naturally lead to a localization of the wave function in the stochastic dynamics considered. Hence, this simple model provides an ideal playground for analyzing temporal structures that are induced by the environment acting on the system.

We consider an open quantum system coupled to a Markovian bath [3, 72], whose dynamics is governed by the Lindblad master equation

$$\frac{d\hat{\rho}}{dt} = -i [\hat{H}, \hat{\rho}] + \sum_j \gamma_j \mathcal{D}[\hat{L}_j](\hat{\rho}). \quad (1)$$

Here, \hat{H} is the Hamiltonian and $\mathcal{D}[\hat{L}_j](\hat{\rho})$ are the dissipators with Lindblad operators \hat{L}_j and dissipation rates γ_j , with the dissipator defined by $\mathcal{D}[\hat{A}](\hat{\rho}) = \hat{A}\hat{\rho}\hat{A}^\dagger - \frac{1}{2}\hat{A}^\dagger\hat{A}\hat{\rho} - \frac{1}{2}\hat{\rho}\hat{A}^\dagger\hat{A}$.

A. Tight-Binding Hamiltonian

We consider a system of free spinless non-interacting electrons on a discrete lattice with N sites, periodic boundary conditions, and nearest-neighbor hopping, modeled by a tight-binding Hamiltonian [73]:

$$\hat{H}_{\text{TB}} = -t_{\text{hop}} \sum_{a=1}^N (\hat{c}_a^\dagger \hat{c}_{a+1} + \hat{c}_{a+1}^\dagger \hat{c}_a), \quad (2)$$

with $\hat{c}_{N+1} = \hat{c}_1$, where t_{hop} is the hopping amplitude. Here, \hat{c}_a^\dagger and \hat{c}_a are the electronic creation and annihilation operators, respectively. The system can be diagonalized in quasi-momentum space, where the Hamiltonian reads:

$$\hat{H}_{\text{TB}} = \sum_k \varepsilon_k \hat{c}_k^\dagger \hat{c}_k, \quad (3)$$

with the momentum space annihilation and creation operators \hat{c}_k and \hat{c}_k^\dagger . In this representation, one obtains the dispersion relation [74]

$$\varepsilon_k = -2t_{\text{hop}} \cos(ka), \quad (4)$$

where a is the lattice constant. As we deal with periodic boundary conditions, the allowed k -values are restricted to the first Brillouin zone ($-\pi/a \leq k < \pi/a$), such that $k = \frac{2\pi}{Na} m$, with $m \in \{-N/2, -N/2 + 1, \dots, N/2 - 1\}$. In the following, we will set the lattice spacing $a = 1$ for simplicity. The set of corresponding quasi-momentum states $\{|k\rangle\}$ represent a complete and orthonormal basis of the systems' Hilbert space.

B. Measurement Interaction

We consider a weak local interaction with the system, resembling continuous measurements of the particle's position around each lattice point. We model the dissipation induced by this environmental interaction using dissipators with quasi-local Lindblad operators acting on the *position* of the particle around a region of a certain lattice point. We consider Hermitian Lindblad operators \hat{D}_a acting around lattice point a :

$$\begin{aligned} \hat{D}_a &= \sum_{b=1}^N h_a(b) \hat{c}_b^\dagger \hat{c}_b \\ &= \frac{1}{N} \sum_{k,k'} \hat{c}_k^\dagger \hat{c}_{k'} \sum_b h_a(b) e^{i(k-k')b}. \end{aligned} \quad (5)$$

Here, $h_a(b)$ is an amplitude function that depends on the distance between the lattice points a and b . The amplitude function $h_a(b)$ of a Lindblad operator \hat{D}_a models the strength and locality of the interaction with the system around a lattice point a , depending only on the spatial distance between two lattice points a and b .

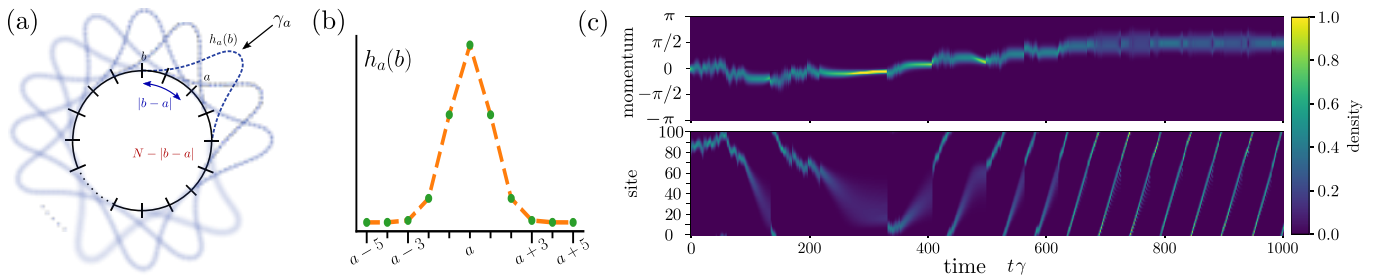


FIG. 1. (a) Schematic representation of the system setup. At each lattice point a , a Lindblad operator acts locally on the system with amplitude function $h_a(b)$, and dissipation rate γ_a . (b) Amplitude function $h_a(b)$ of the Lindblad operator \hat{D}_a for constant lattice point a and $\sigma = 1$. (c) Probability density of a sample trajectory as a function of time in quasi-momentum (top) and real space representation (bottom). System parameters: $\gamma_a = t_{\text{hop}} \forall a$, $N = 100$, $\sigma = 0.1N$; initial state: $\hat{\rho}_0 = |k_0\rangle\langle k_0| = |0\rangle\langle 0|$. Due to the measurement-induced interaction, the particle starts moving along the chain in a sustained periodic motion.

As a result, measuring the particle will result in the localization of its position. Repeated weak measurements of an initial delocalized particle will further localize the particle's wave function.

Due to the periodic boundary conditions, the amplitude function $h_a(b)$ needs to incorporate both distances, $|a-b|$ and $N-|a-b|$. We consider $h_a(b)$ having a Gaussian form:

$$h_a(b) = \frac{1}{\sqrt{N_h}} \left(e^{-\frac{1}{2}\left(\frac{b-a}{\sigma}\right)^2} + e^{-\frac{1}{2}\left(\frac{N-|b-a|}{\sigma}\right)^2} \right), \quad (6)$$

with the variance σ^2 characterizing the width of the Gaussian and a normalization constant N_h which is chosen such that:

$$\langle \psi | \sum_{a=1}^N \hat{D}_a^\dagger \hat{D}_a | \psi \rangle = 1, \quad (7)$$

for any arbitrary state $|\psi\rangle$. This requirement fixes the normalization:

$$\sum_{a=1}^N h_a^2(b) = 1 \quad \forall b \in [1, \dots, N] \quad (8)$$

The variance σ^2 describes the broadening of the amplitude function $h_a(b)$ around lattice point a and is thus directly related to the uncertainty of the Lindblad operator \hat{D}_a : For larger values of σ , the operators \hat{D}_a will induce a larger delocalization on the lattice and correspondingly a stronger localization in quasi-momentum space. The amplitude function $h_a(b)$ is schematically depicted in Fig. 1(b).

To express \hat{D}_a in the quasi-momentum basis, we compute the discrete Fourier transform of $h_a(b)$:

$$\mathcal{F}[h_a(b)](q) = \frac{1}{\sqrt{N}} \sum_{b=1}^N h_a(b) e^{iqb} \equiv \eta(q) e^{-iqa}, \quad (9)$$

where we have defined $\eta(q) \equiv \mathcal{F}[h_0(b)](q)$. Eq. (5) then becomes

$$\hat{D}_a = \frac{1}{\sqrt{N}} \sum_{k,k'} \hat{c}_k^\dagger \hat{c}_{k'} \eta(k-k') e^{-ia(k-k')}. \quad (10)$$

With the system Hamiltonian \hat{H}_{TB} and the Lindblad operators \hat{D}_a , the Lindblad master equation reads

$$\frac{d}{dt} \hat{\rho} = -i[\hat{H}_{\text{TB}}, \hat{\rho}] + \sum_{a=1}^N \gamma_a \mathcal{D}[\hat{D}_a](\hat{\rho}). \quad (11)$$

The rates γ_a are real positive coefficients representing the *dampening* amplitude of the corresponding damping channel for the Lindblad operators \hat{D}_a each acting locally a region around a lattice point a .

III. RESULTS

We now turn to results obtained from direct numerical integration of the Lindblad master equation and obtained from the quantum trajectory method. In Fig. 1(c), we show a sample quantum trajectory for an initially fully delocalized state. We observe the emergence of a sustained periodic motion and localization of wave function induced by dissipation.

A. Equations of Motion

We can express the Lindblad master equation as a super-operator \mathcal{L} acting on the system's density matrix $\hat{\rho}$:

$$\frac{d}{dt} \rho_{kk'} |k\rangle\langle k'| = \sum_{\alpha\beta} \mathcal{L}_{kk'\alpha\beta} \rho_{\alpha\beta} |\alpha\rangle\langle\beta|. \quad (12)$$

Explicitly computing the matrix elements of the Liouvillian leads to the following explicit form of the Lindblad

master equation [See Appendix A for detailed derivation]:

$$\begin{aligned} \mathcal{L}[\rho_{kk'}] &= -i(\varepsilon_k - \varepsilon_{k'}) \rho_{kk'} \\ &+ \frac{1}{N} \sum_a \gamma_a \left\{ \sum_{\alpha, \beta} \left[\eta(\alpha - k) \eta(k' - \beta) e^{-ia(\alpha - \beta + k' - k)} \rho_{\alpha\beta} \right. \right. \\ &\quad - \frac{1}{2} \eta(\alpha - \beta) \eta(\beta - k) e^{-ia(\alpha - k)} \rho_{\alpha k'} \\ &\quad \left. \left. - \frac{1}{2} \eta(k' - \alpha) \eta(\alpha - \beta) e^{-ia(k' - \beta)} \rho_{k\beta} \right] \right\}. \end{aligned} \quad (13)$$

In the case of all Lindblad operators acting on the system with equal dissipation rates, i.e. $\gamma_a = \gamma = \text{const.}$, the above equation reduces to:

$$\begin{aligned} \mathcal{L}[\rho_{kk'}] &= [-i(\varepsilon_k - \varepsilon_{k'}) - \gamma] \rho_{kk'} \\ &+ \gamma \sum_{\alpha, \beta} \eta(\alpha - k) \eta(k' - \beta) \delta_{\alpha - \beta, k - k'} \rho_{\alpha\beta}. \end{aligned} \quad (14)$$

In the following, we consider the case in which all Lindblad operators \hat{D}_a act on the system with equal dissipation rates $\gamma_a = \gamma$. This resembles the physical situation in which each lattice point interacts equally with its surrounding environment.

With an initially mixed density $\hat{\rho}_0 = \sum_k \rho_{kk} |k\rangle\langle k|$, the time-evolved density matrix remains diagonal and real at all times. The time-evolution of the diagonal elements is then given by [See Appendix B for detailed derivation]

$$\frac{d}{dt} \rho_{kk} = \gamma \left(\sum_{\alpha} \eta^2(\alpha - k) \rho_{\alpha\alpha} - \rho_{kk} \right). \quad (15)$$

The above equation is a coupled linear differential equation and can be solved by diagonalizing $\mathcal{L}_{\alpha k} = \eta^2(\alpha - k) - \delta_{\alpha k}$. Together with the numerical result, the exact solution to the above equation is shown in Fig. 2 for an initial pure state with zero-quasi-momentum $\hat{\rho} = |k=0\rangle\langle k=0|$. The resulting steady state is an equilibrium state corresponding to infinite temperature where each quasi-momentum state is equally occupied.

B. Two-Time Correlations

We now consider the two-time correlator of the Lindblad operator \hat{D}_a :

$$C_a(t, \tau) = \langle \hat{D}_a^\dagger(t + \tau) \hat{D}_a(t) \rangle. \quad (16)$$

To analyze temporal structures in the steady state, we calculate $C_a(t, \tau)$ for $t \rightarrow \infty$. In this limit, we have

$$\lim_{t \rightarrow \infty} C_a(t, \tau) = \langle \hat{D}_a^\dagger(\tau) \hat{D}_a \rangle_{\text{ss}} = \frac{1}{N} \text{Tr} \left\{ \hat{D}_a^\dagger(\tau) \hat{D}_a \right\}, \quad (17)$$

where in the last step, we have used the fact that the steady state is a maximally mixed state corresponding

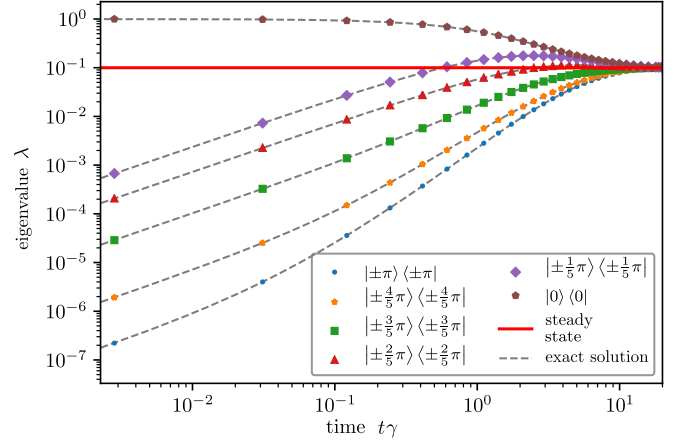


FIG. 2. Diagonal matrix elements of the density matrix $\hat{\rho}$ as a function of time for $N = 10$ sites. The markers indicate simulation results from direct numerical integration. Here, the system is initialized with $\hat{\rho} = |k_0\rangle\langle k_0| = |0\rangle\langle 0|$.

to infinite temperature. Taking the limit of $\tau \rightarrow \infty$, in Eq. (17), the operators decorrelate, yielding

$$\lim_{\tau \rightarrow \infty} \langle \hat{D}_a^\dagger(\tau) \hat{D}_a \rangle_{\text{ss}} = \langle \hat{D}_a \rangle_{\text{ss}}^2 = \frac{1}{N^2} \text{Tr} \left\{ \hat{D}_a \right\}^2, \quad (18)$$

where we have used that \hat{D}_a is Hermitian. We construct the normalized correlation function

$$C_{a,ss}(\tau) = \frac{\langle \hat{D}_a(\tau) \hat{D}_a \rangle_{\text{ss}} - \langle \hat{D}_a \rangle_{\text{ss}}^2}{\langle \hat{D}_a(0) \hat{D}_a \rangle_{\text{ss}} - \langle \hat{D}_a \rangle_{\text{ss}}^2}. \quad (19)$$

With this definition, $C_{a,ss}(0) = 1$ and $C_{a,ss}(\tau \rightarrow \infty) = 0$.

The correlation function $C_{a,ss}(\tau)$ is shown in Fig. 3(a) for various dissipation rates γ . We observe that correlations in $C_{a,ss}(\tau)$ are present even in the steady state with

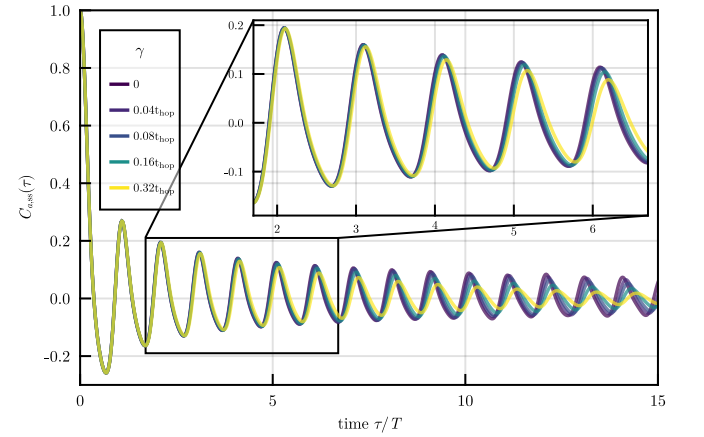


FIG. 3. Steady state correlation function $C_{a,ss}(\tau)$ as a function of correlation time τ in units of period T corresponding to maximum group velocity for different dissipation rates γ . $\sigma = 0.1N$, $N = 200$.

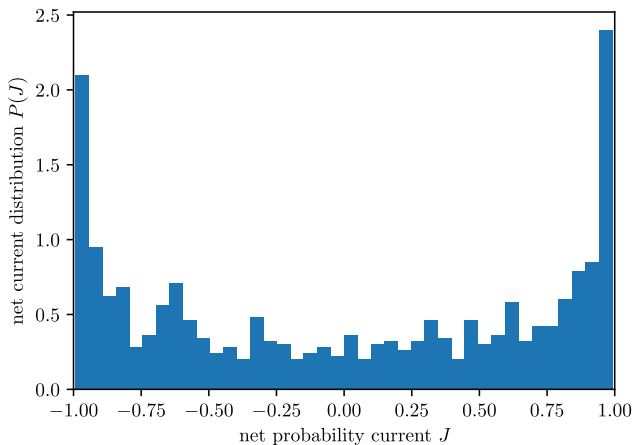


FIG. 4. Distribution density of the net probability current J for $N_{\text{traj}} = 1000$ trajectories at $t = 500\gamma$ with $|\psi_{\text{init}}\rangle = |k = 0\rangle$. System parameters: $N = 100$, $t_{\text{hop}} = 25\gamma$, $\sigma = 0.1N$.

a damped periodicity close to the period T corresponding to maximum group velocity $v_g = 2t_{\text{hop}}$. The quantum trajectory method provides an intuitive interpretation of this non-trivial behavior: Due to subsequent Lindblad operators acting on the system, the wave function becomes localized in space, asymptotically approaching a state centered around $|k\rangle = |\pm \frac{\pi}{2}\rangle$. We observe leading dynamics in each quantum trajectory where the localized wave function moves around the ring with a velocity close to the maximum group velocity. As a change of direction of the wave function in individual quantum trajectories is not forbidden by symmetries and does occur randomly on a characteristic time scale, the steady state correlation function in $C_{a,\text{ss}}(\tau)$ decays eventually.

C. Probability Density Current

We consider the current operator \hat{j}_a between two sites a and $a + 1$:

$$\hat{j}_a = -i(\hat{c}_{a+1}^\dagger \hat{c}_a - \hat{c}_a^\dagger \hat{c}_{a+1}) \quad (20)$$

Using the relation $\text{Im}(z) = -i(z - z^*)/2$, the probability current of state $|\psi\rangle$ at site a is given by

$$\langle \hat{j}_a \rangle = 2\text{Im}(\langle \psi | \hat{c}_a^\dagger \hat{c}_{a+1} | \psi \rangle). \quad (21)$$

Summing over all sites we obtain the net probability current $J(t)$ as a function of time:

$$J(t) = \sum_{a=1}^N \text{Im}(\langle \hat{c}_a^\dagger \hat{c}_{a+1} \rangle) \quad (22)$$

In the steady state, the probability current expectation value vanishes, characterizing an equilibrium. To see this, we calculate the current operator in quasi-momentum representation in which it takes the form

$$\langle k | \hat{j}_a | k \rangle = 2 \sin(k). \quad (23)$$

Calculating the expectation value $\langle \hat{j}_a \rangle$ in the steady state, we obtain

$$\begin{aligned} \langle \hat{j}_a \rangle_{\text{ss}} &= \text{Tr}\{\hat{j}_a \hat{\rho}_{\text{ss}}\} = \frac{1}{N} \sum_k \langle k | \hat{j}_a | k \rangle \\ &= \frac{1}{N} \sum_k 2 \sin(k) = 0. \end{aligned} \quad (24)$$

In the steady state, no spatial direction to which the wave-function moves is preferred, and therefore, we observe a symmetric bimodal distribution in the net probability current in the quantum trajectories at the steady state which we show in Fig. 4.

D. Inverse Participation Ratio

To analyze the degree of *localization* of the wave function in individual quantum trajectories, we define the inverse participation ratio in spatial basis [75]:

$$\begin{aligned} \text{IPR}(|\psi\rangle) &= \frac{1}{\sum_i |\langle i | \psi \rangle|^4} = \begin{cases} N & \text{for } |\psi\rangle \text{ fully extended} \\ 1 & \text{for } |\psi\rangle \text{ fully localized} \end{cases} \end{aligned} \quad (25)$$

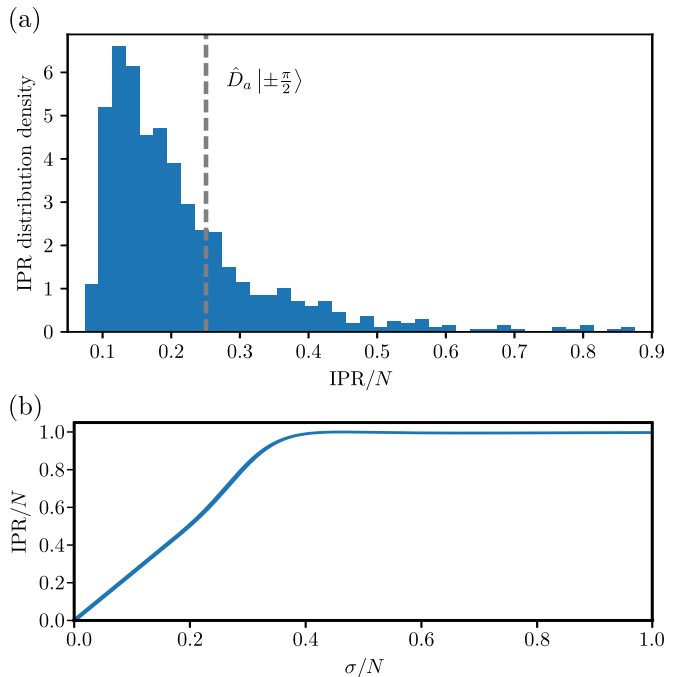


FIG. 5. (a) Distribution density of the IPR for $N_{\text{traj}} = 1000$ trajectories at $t = 500\gamma$ for an initial state $|\psi_{\text{init}}\rangle = |k = \pi/2\rangle$. System parameters: $N = 100$, $\sigma = 0.1N$, $t_{\text{hop}} = N\gamma/4$. (b) IPR as function of the width σ of the amplitude function $h_a(b)$, associated with Lindblad operator \hat{D}_a for a state $\hat{D}_a |k\rangle$.

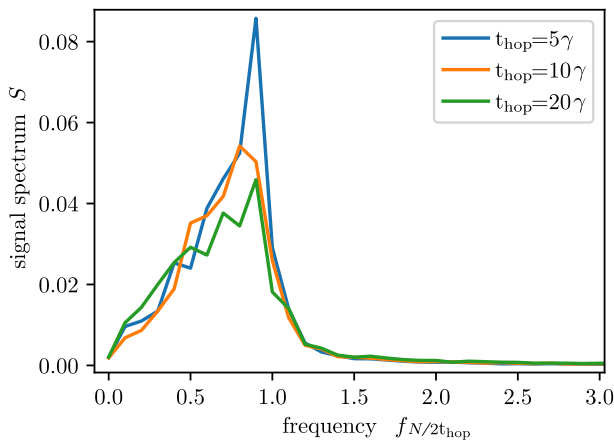


FIG. 6. Power spectral density S for single quantum trajectories in the long-time limit for different hopping amplitudes t_{hop} .

where $\{|i\rangle\}$ is the spatial basis of the system. The system naturally exhibits localization due to the subsequent quantum jumps at different sites as shown in Fig. 5(a).

The IPR for a state with a Lindblad operator \hat{D}_a acting on an arbitrary quasi-momentum state is given by

$$\text{IPR}(\hat{D}_a |k\rangle) = 1/\sum_b h_a^4(b), \quad (26)$$

and thus depends on the width σ of the amplitude function $h_a(b)$, as shown in Fig. 5(b).

E. Time-Domain Frequency Analysis

To analyze the involved frequencies in the quantum trajectory dynamics, we look at the position of the peak amplitude of the localized wave-function. We parameterize the position of the peak amplitude by a discrete angle $\phi_j = (2\pi j/N \bmod N)$ on the ring. Projecting the angle onto the y -axis, $y(t) = \sin(\phi(t))$, we obtain a quasi-periodic signal. To quantify involved frequencies in the motion of the peak amplitude position around the ring, we compute the power spectral density, defined by a discrete Fourier transform in the time domain [76]:

$$S(\omega) = \frac{\Delta t^2}{T} \left| \sum_{j=1}^{N_t} y_j e^{-i\omega j \Delta t} \right|^2, \quad (27)$$

where N_t is the total number of timesteps for the considered quantum trajectory and y_j is the projection on the y -axis for the j -th timestep.

Computing the power spectral density in the long-time limit of individual quantum trajectories, we observe a peak signal at the frequency corresponding to the maximal group velocity of the system Hamiltonian $v_g = \pm 2t_{\text{hop}}$, as shown in Fig. 6.

IV. CONCLUSION

In this work, we have considered a measurement-induced clock in an open quantum system of non-interacting electrons on a periodic lattice, circumventing the requirement of external drives or many-body interactions.

(i) Individual trajectories exhibit wave-function localization due to successive quantum jumps of Lindblad operators modeling continuous quasi-local position measurements of the system. In the steady state, the wave function is found symmetric around quasi-momentum states $|k\rangle = |\pm \frac{\pi}{2}\rangle$, corresponding to the maximum group velocity $v_g = \pm 2t_{\text{hop}}$. The interplay between the dissipation rate γ and the amplitude function's width σ significantly dictates the timescale of unidirectional motion of the wave packet.

(ii) We observe a damped periodicity of two-time expectation values in the steady-state, matching the periodicity of maximum group velocity. The oscillations are sustained for a time scale associated with the dissipation rate γ and hopping amplitude t_{hop} . In the steady state, the net probability density current admits a bimodal distribution, indicating the motion of the particle clock-wise or counter-clock-wise around the ring. Furthermore, using a time-series analysis of the peak-amplitude position of the wave function, we reveal a dominant frequency associated with the particle's motion.

This decaying time-periodic structure, exhibited in the steady state of this chain of non-interacting electrons with measurement-induced interaction, is broadly applicable across a wide parameter range, indicating its robustness and generality. These results may have potential implications for the design of robust quantum clocks.

ACKNOWLEDGMENTS

D.S. acknowledges support by the Swiss National Science Foundation through Projects No. 200020_185015 and 200020_215172. S.K. acknowledges partial support through the Deutsche Forschungsgemeinschaft (DFG, German Research Foundation) via Research Unit FOR 2414 under project number 277974659, and by the National Science Foundation under Grants No. NSF PHY-1748958 and PHY-2309135.

Appendix A: Derivation of the Liouvillian Equations of Motion

Here, we give a detailed derivation of the Liouvillian equation of motion in Eq. (13) in the main text. The master equation for the density matrix $\hat{\rho}$ is given by [c.f. Eq. (11) in the main text]

$$\frac{d}{dt} \hat{\rho} = -i[\hat{H}_{\text{TB}}, \hat{\rho}] + \sum_{a=1}^N \gamma_a \mathcal{D}[\hat{D}_a](\hat{\rho}), \quad (\text{A1})$$

where \hat{H}_{TB} is the tight-binding Hamiltonian of the system, defined in Eq. (2) and \hat{D}_a are the Lindblad operators, defined in Eq. (5). The dissipator $\mathcal{D}[\hat{A}]$ of a Lindblad operator \hat{A} is defined by

$$\mathcal{D}[\hat{A}](\hat{\rho}) \equiv \hat{A}\hat{\rho}\hat{A}^\dagger - \frac{1}{2}\hat{A}^\dagger\hat{A}\hat{\rho} - \frac{1}{2}\hat{\rho}\hat{A}^\dagger\hat{A}. \quad (\text{A2})$$

We express the Lindblad master equation as a super-operator \mathcal{L} acting on the system's density matrix $\hat{\rho}$:

$$\frac{d}{dt}\rho_{kk'} |k\rangle\langle k'| = \sum_{\alpha\beta} \mathcal{L}_{kk'\alpha\beta} \rho_{\alpha\beta} |\alpha\rangle\langle\beta|. \quad (\text{A3})$$

To calculate the different matrix elements of the Liouvillian, we first look at the unitary part of Eq. (11):

$$\begin{aligned} -i[\hat{H}_{\text{TB}}, |k\rangle\langle k'|] &= -i \left[\sum_{\alpha} \varepsilon_{\alpha} \hat{c}_{\alpha}^{\dagger} \hat{c}_{\alpha}, |k\rangle\langle k'| \right] \\ &= -i \left(\sum_{\alpha} \varepsilon_{\alpha} \hat{c}_{\alpha}^{\dagger} \hat{c}_{\alpha} |k\rangle\langle k'| - |k\rangle\langle k'| \sum_{\alpha} \varepsilon_{\alpha} \hat{c}_{\alpha}^{\dagger} \hat{c}_{\alpha} \right) \quad (\text{A4}) \\ &= -i (\varepsilon_k |k\rangle\langle k'| - |k\rangle\langle k'| \varepsilon_{k'}) \\ &= -i (\varepsilon_k - \varepsilon_{k'}) |k\rangle\langle k'| \end{aligned}$$

It is important to note that the Lindblad operators \hat{D}_a are Hermitian, and hence the dissipator reduces to

$$\mathcal{D}[\hat{D}_a](\hat{\rho}) \equiv \hat{D}_a \hat{\rho} \hat{D}_a - \frac{1}{2} \hat{D}_a^2 \hat{\rho} - \frac{1}{2} \hat{\rho} \hat{D}_a^2. \quad (\text{A5})$$

Considering the first part of the dissipator, we compute

$$\begin{aligned} &\hat{D}_a |k\rangle\langle k'| \hat{D}_a \\ &= \frac{1}{N} \left(\sum_{\alpha, \alpha'} \hat{c}_{\alpha}^{\dagger} \hat{c}_{\alpha'} \eta(\alpha - \alpha') e^{-ia(\alpha - \alpha')} \right) |k\rangle\langle k'| \\ &\quad \times \left(\sum_{\beta, \beta'} \hat{c}_{\beta}^{\dagger} \hat{c}_{\beta'} \eta(\beta - \beta') e^{-ia(\beta - \beta')} \right) \\ &= \frac{1}{N} \left(\sum_{\alpha, \alpha'} \hat{c}_{\alpha}^{\dagger} \delta_{\alpha'k} \eta(\alpha - \alpha') e^{-ia(\alpha - \alpha')} \right) |\Omega\rangle\langle\Omega| \\ &\quad \times \left(\sum_{\beta, \beta'} \delta_{\beta k'} \hat{c}_{\beta'} \eta(\beta - \beta') e^{-ia(\beta - \beta')} \right) \\ &= \frac{1}{N} \left(\sum_{\alpha} \eta(\alpha - k) e^{-ia(\alpha - k)} |\alpha\rangle \right) \\ &\quad \times \left(\langle\beta'| \sum_{\beta'} \eta(k' - \beta') e^{-ia(k' - \beta')} \right) \\ &= \frac{1}{N} \sum_{\alpha, \beta} \eta(\alpha - k) \eta(k' - \beta) e^{-ia(\alpha - \beta + k' - k)} |\alpha\rangle\langle\beta|, \quad (\text{A6}) \end{aligned}$$

where $|\Omega\rangle$ is the vacuum state.

For $\hat{D}_a^2 \hat{\rho}$, we get

$$\begin{aligned} &\hat{D}_a^2 |k\rangle\langle k'| \\ &= \frac{1}{N} \sum_{\alpha, \alpha', \beta, \beta'} \left(\hat{c}_{\alpha}^{\dagger} \hat{c}_{\alpha'} \hat{c}_{\beta}^{\dagger} \hat{c}_{\beta'} \eta(\alpha - \alpha') e^{-ia(\alpha - \alpha')} \right. \\ &\quad \left. \times \eta(\beta - \beta') e^{-ia(\beta - \beta')} |k\rangle\langle k'| \right) \\ &= \frac{1}{N} \sum_{\alpha, \alpha', \beta, \beta'} \left(\delta_{\alpha' \beta} \delta_{\beta' k} \eta(\alpha - \alpha') \eta(\beta - \beta') \right. \\ &\quad \left. \times e^{-ia(\alpha - \alpha' + \beta - \beta')} |\alpha\rangle\langle k'| \right) \quad (\text{A7}) \\ &= \frac{1}{N} \sum_{\alpha, \beta} \eta(\alpha - \beta) \eta(\beta - k) e^{-ia(\alpha - k)} |\alpha\rangle\langle k'|. \end{aligned}$$

Analogous for $|k\rangle\langle k'| \hat{D}_a^2$:

$$\begin{aligned} &|k\rangle\langle k'| \hat{D}_a^2 \\ &= \frac{1}{N} \sum_{\alpha, \alpha', \beta, \beta'} \left(|k\rangle\langle k'| \hat{c}_{\alpha}^{\dagger} \hat{c}_{\alpha'} \hat{c}_{\beta}^{\dagger} \hat{c}_{\beta'} \right. \\ &\quad \left. \times \eta(\alpha - \alpha') e^{-ia(\alpha - \alpha')} \right. \\ &\quad \left. \times \eta(\beta - \beta') e^{-ia(\beta - \beta')} \right) \\ &= \frac{1}{N} \sum_{\alpha, \alpha', \beta, \beta'} \left(|k\rangle\langle\beta'| \delta_{k' \alpha} \delta_{\alpha' \beta} \eta(\alpha - \alpha') \eta(\beta - \beta') \right. \quad (\text{A8}) \\ &\quad \left. \times e^{-ia(\alpha - \alpha' + \beta - \beta')} \right) \\ &= \frac{1}{N} \sum_{\beta, \beta'} \eta(k' - \beta) \eta(\beta - \beta') e^{-ia(k' - \beta')} |k\rangle\langle\beta'| \\ &= \frac{1}{N} \sum_{\alpha, \beta} \eta(k' - \alpha) \eta(\alpha - \beta) e^{-ia(k' - \beta)} |k\rangle\langle\beta|, \end{aligned}$$

where in the last step, we have just renamed variables. Thus, the Lindblad master equation is explicitly given by Eq. (13):

$$\begin{aligned} \mathcal{L}[\rho_{kk'}] &= \\ &-i(\varepsilon_k - \varepsilon_{k'}) \rho_{kk'} \\ &+ \frac{1}{N} \sum_a \gamma_a \left\{ \sum_{\alpha, \beta} \left[\eta(\alpha - k) \eta(k' - \beta) \right. \right. \\ &\quad \left. \left. \times e^{-ia(\alpha - \beta + k' - k)} \rho_{\alpha\beta} \right. \right. \\ &\quad \left. \left. - \frac{1}{2} \eta(\alpha - \beta) \eta(\beta - k) e^{-ia(\alpha - k)} \rho_{\alpha k'} \right. \right. \\ &\quad \left. \left. - \frac{1}{2} \eta(k' - \alpha) \eta(\alpha - \beta) e^{-ia(k' - \beta)} \rho_{k\beta} \right] \right\}. \quad (\text{A9}) \end{aligned}$$

In the case of all Lindblad operators acting on the system with equal dissipation rates, i.e. $\gamma_a = \gamma = \text{const.}$, the above equation reduces to [c.f Eq. (14) in the main

text]:

$$\begin{aligned} \mathcal{L}[\rho_{kk'}] &= [-i(\varepsilon_k - \varepsilon_{k'}) - \gamma] \rho_{kk'} \\ &+ \gamma \sum_{\alpha\beta} \eta(\alpha - k) \eta(k' - \beta) \delta_{\alpha-\beta, k-k'} \rho_{\alpha\beta}. \end{aligned} \quad (\text{A10})$$

It is straightforward to check that the above equation of motion for the matrix elements $\rho_{kk'}$ preserves trace and Hermiticity of $\hat{\rho}$.

Appendix B: Derivation of the Exact result

Here, we prove that for an initially mixed density matrix with $\hat{\rho}_0 = \sum_k \rho_{kk} |k\rangle\langle k|$, the time evolved density matrix remains diagonal and real at all times. The time-evolution of the diagonal elements is given by [c.f Eq. (15) in the main text]

$$\frac{d}{dt} \rho_{kk} = \mathcal{L}[\hat{\rho}] = \gamma \left(\sum_{\alpha=1}^N \eta^2(\alpha - k) \rho_{\alpha\alpha} - \rho_{kk} \right), \quad (\text{B1})$$

Proof: The unitary term in the Liouvillian is only nonzero for $k \neq k'$ and thus zero at all times for any initial mixed state. The Liouvillian thus becomes:

$$\begin{aligned} \mathcal{L}[\hat{\rho}] &= \frac{1}{N} \gamma \sum_{a=1}^N \left\{ \sum_{\alpha,\beta} \left[\eta(\alpha - k) \eta(k' - \beta) e^{-ia(\alpha-\beta+k'-k)} \rho_{\alpha\beta} \right. \right. \\ &\quad - \frac{1}{2} \eta(\alpha - \beta) \eta(\beta - k) e^{-ia(\alpha-k)} \rho_{\alpha k'} \\ &\quad \left. \left. - \frac{1}{2} \eta(k' - \alpha) \eta(\alpha - \beta) e^{-ia(k'-\beta)} \rho_{k,\beta} \right] \right\} \end{aligned} \quad (\text{B2})$$

By assumption of the initial state, only diagonal matrix elements contribute to the Liouvillian:

$$\begin{aligned} \mathcal{L}[\hat{\rho}] &= \frac{1}{N} \gamma \sum_{a=1}^N \left\{ \sum_{\alpha,\beta} \left[\eta(\alpha - k) \eta(k' - \alpha) e^{-ia(k'-k)} \rho_{\alpha\alpha} \right. \right. \\ &\quad - \frac{1}{2} \eta(k' - \beta) \eta(\beta - k) e^{-ia(k'-k)} \rho_{k',k'} \\ &\quad \left. \left. - \frac{1}{2} \eta(k' - \alpha) \eta(\alpha - k) e^{-ia(k'-k)} \rho_{kk} \right] \right\}. \end{aligned} \quad (\text{B3})$$

Since each of the phase factors are equal, summing over a yields only contributions for $k' = k$:

$$\begin{aligned} \mathcal{L}[\hat{\rho}] &= \frac{1}{N} \gamma \sum_{\alpha,\beta} \left[\eta^2(\alpha - k) \rho_{\alpha\alpha} \right. \\ &\quad \left. - \frac{1}{2} (\eta^2(\beta - k) + \eta^2(\alpha - k)) \rho_{kk} \right]. \end{aligned} \quad (\text{B4})$$

Summing over α and β , and recalling that $\sum_k \eta^2(k - k') = 1$ [See Eq. (8)], we are left with

Eq. (B1), which proofs the identity of Eq. (15). We recognize that the fully mixed state $\hat{\rho} = \sum_k \frac{1}{N} |k\rangle\langle k|$ is a fixpoint of the Lindblad master equation since for this state $\mathcal{L}[\hat{\rho}] = 0$.

Appendix C: Sample Trajectories

In Fig. 7, we plot various sample trajectories both in quasi-momentum space and position space for different system parameters γ , and σ for a system size of $N = 100$.

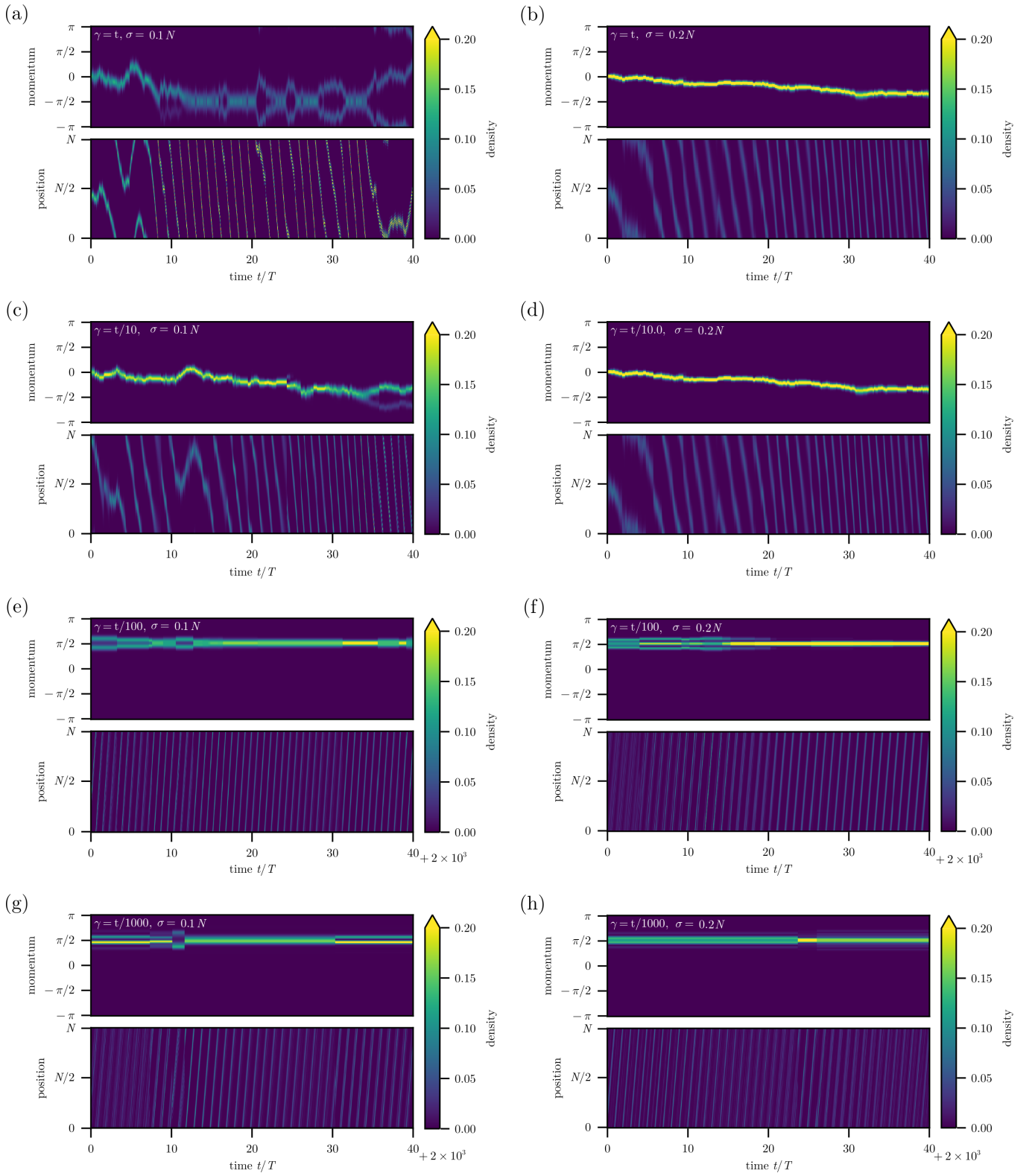


FIG. 7. (a-h) Sample trajectories for different system parameters γ, σ as a function of normalized time t/T , where T is the time period associated with maximum group velocity v_g . (e-h) For small dissipation rates, $\gamma \ll t_{\text{hop}}$, we show the trajectories after the transient dynamics after time $t = 2 \times 10^3 T$. All trajectories are initialized with a fully delocalized state, $|\psi_0\rangle \propto \sum_{n=0}^{N-1} |n\rangle$.

-
- [1] U. Weiss, *Quantum Dissipative Systems* (WORLD SCIENTIFIC, 2011).
- [2] A. Rivas and S. F. Huelga, *Open quantum systems : an introduction* (Springer, 2012) p. 97.
- [3] H.-P. Breuer and F. Petruccione, *The Theory of Open Quantum Systems* (Oxford University Press, 2015).
- [4] C. Macchiavello, G. M. Palma and A. Zeilinger, *Quantum Computation and Quantum Information Theory* (Cambridge University Press, 2001) p. 676.
- [5] M. Schlosshauer, *Decoherence and the Quantum-To-Classical Transition*, Frontiers Collection (Springer Berlin Heidelberg, Berlin, Heidelberg, 2007).
- [6] G. Schaller, *Open Quantum Systems Far from Equilibrium*, Lecture Notes in Physics, Vol. 881 (Springer International Publishing, Cham, 2014).
- [7] G. M. Palma, K.-a. Suominen and A. Ekert, *Quantum computers and dissipation*, *Proceedings of the Royal Society of London. Series A: Mathematical, Physical and Engineering Sciences* **452**, 567 (1996).
- [8] W. H. W. H. Louisell, *Quantum statistical properties of radiation* (Wiley, 1973) p. 528.
- [9] C. Cohen-Tannoudji, J. Dupont-Roc and G. Grynberg, *Atom-Photon Interactions: Basic Processes and Applications* (EDP Sciences, 1998).
- [10] H. Carmichael, *Statistical methods in quantum optics 2 : non-classical fields* (Springer, 2008) p. 540.
- [11] A. Szameit and S. Nolte, *Discrete optics in femtosecond-laser-written photonic structures*, *Journal of Physics B: Atomic, Molecular and Optical Physics* **43**, 163001 (2010).
- [12] I. Bloch, J. Dalibard and W. Zwerger, *Many-body physics with ultracold gases*, *Rev. Mod. Phys.* **80**, 885 (2008).
- [13] F. Dimer, B. Estienne, A. S. Parkins and H. J. Carmichael, *Proposed realization of the Dicke-model quantum phase transition in an optical cavity QED system*, *Phys. Rev. A* **75**, 013804 (2007).
- [14] K. Baumann, C. Guerlin, F. Brennecke and T. Esslinger, *Dicke quantum phase transition with a superfluid gas in an optical cavity*, *Nature* **464**, 1301 (2010).
- [15] K. Baumann, R. Mottl, F. Brennecke and T. Esslinger, *Exploring Symmetry Breaking at the Dicke Quantum Phase Transition*, *Phys. Rev. Lett.* **107**, 140402 (2011).
- [16] F. Brennecke, R. Mottl, K. Baumann, R. Landig, T. Donner and T. Esslinger, *Real-time observation of fluctuations at the driven-dissipative Dicke phase transition*, *Proceedings of the National Academy of Sciences* **110**, 11763 (2013).
- [17] A. J. Leggett, S. Chakravarty, A. T. Dorsey, M. P. A. Fisher, A. Garg and W. Zwerger, *Dynamics of the dissipative two-state system*, *Reviews of Modern Physics* **59**, 1 (1987).
- [18] K. Blum, *Density Matrix Theory and Applications* (Springer US, Boston, MA, 1996).
- [19] S. Dattagupta and P. Sanjay, *Dissipative phenomena in condensed matter*, 2004th ed., Springer Series in Materials Science (Springer, Berlin, Germany, 2004).
- [20] M. Fitzpatrick, N. M. Sundaresan, A. C. Y. Li, J. Koch and A. A. Houck, *Observation of a Dissipative Phase Transition in a One-Dimensional Circuit QED Lattice*, *Phys. Rev. X* **7**, 011016 (2017).
- [21] S. A. Sato, J. W. McIver, M. Nuske, P. Tang, G. Jotzu, B. Schulte, H. Hübener, U. De Giovannini, L. Mathey, M. A. Sentef, A. Cavalleri and A. Rubio, *Microscopic theory for the light-induced anomalous Hall effect in graphene*, *Phys. Rev. B* **99**, 214302 (2019).
- [22] J. W. McIver, B. Schulte, F.-U. Stein, T. Matsuyama, G. Jotzu, G. Meier and A. Cavalleri, *Light-induced anomalous Hall effect in graphene*, *Nature Physics* **16**, 38 (2019).
- [23] V. May and O. Kühn, *Charge and Energy Transfer Dynamics in Molecular Systems* (Wiley-VCH Verlag GmbH & Co. KGaA, Weinheim, Germany, 2011).
- [24] A. Nitzan, *Chemical dynamics in condensed phases : relaxation, transfer, and reactions in condensed molecular systems* (Oxford University Press, New York, 2006) p. 719.
- [25] M. A. Nielsen and I. L. Chuang, *Quantum Computation and Quantum Information* (Cambridge University Press, Cambridge, England, 2010).
- [26] J. Jin, A. Biella, O. Viyuela, L. Mazza, J. Keeling, R. Fazio and D. Rossini, *Cluster Mean-Field Approach to the Steady-State Phase Diagram of Dissipative Spin Systems*, *Physical Review X* **6**, 031011 (2016).
- [27] E. M. Kessler, G. Giedke, A. Imamoglu, S. F. Yelin, M. D. Lukin and J. I. Cirac, *Dissipative phase transition in a central spin system*, *Physical Review A* **86**, 012116 (2012).
- [28] S. Diehl, A. Tomadin, A. Micheli, R. Fazio and P. Zoller, *Dynamical Phase Transitions and Instabilities in Open Atomic Many-Body Systems*, *Physical Review Letters* **105**, 015702 (2010).
- [29] V. Khemani, A. Lazarides, R. Moessner and S. Sondhi, *Phase Structure of Driven Quantum Systems*, *Physical Review Letters* **116**, 250401 (2016).
- [30] F. Minganti, A. Biella, N. Bartolo and C. Ciuti, *Spectral theory of Liouvillians for dissipative phase transitions*, *Phys. Rev. A* **98**, 042118 (2018).
- [31] Y. L. Dong, T. Neupert, R. Chitra and S. Schmidt, *Signatures of topological quantum phase transitions in driven and dissipative qubit arrays*, *Physical Review B* **94**, 035441 (2016).
- [32] P. St-Jean, V. Goblot, E. Galopin, A. Lemaître, T. Ozawa, L. Le Gratiet, I. Sagnes, J. Bloch and A. Amo, *Lasing in topological edge states of a one-dimensional lattice*, *Nature Photonics* **11**, 651 (2017).
- [33] L. Lu, J. D. Joannopoulos and M. Soljačić, *Topological photonics*, *Nature Photonics* **8**, 821 (2014).
- [34] K. Snizhko, R. Egger and Y. Gefen, *Non-Abelian Berry phase for open quantum systems: Topological protection versus geometric dephasing*, *Physical Review B* **100**, 085303 (2019).
- [35] C.-E. Bardyn, M. A. Baranov, C. V. Kraus, E. Rico, A. Imamoglu, P. Zoller and S. Diehl, *Topology by dissipation*, *New Journal of Physics* **15**, 085001 (2013).
- [36] F. Wilczek, *Quantum Time Crystals*, *Physical Review Letters* **109**, 160401 (2012).
- [37] P. Bruno, *Impossibility of Spontaneously Rotating Time Crystals: A No-Go Theorem*, *Physical Review Letters* **111**, 070402 (2013).
- [38] H. Watanabe and M. Oshikawa, *Absence of Quantum Time Crystals*, *Physical Review Letters* **114**, 251603

- (2015).
- [39] K. Sacha, *Modeling spontaneous breaking of time-translation symmetry*, *Physical Review A* **91**, 033617 (2015).
- [40] D. V. Else, B. Bauer and C. Nayak, *Floquet Time Crystals*, *Physical Review Letters* **117**, 090402 (2016).
- [41] A. Syrwid, J. Zakrzewski and K. Sacha, *Time Crystal Behavior of Excited Eigenstates*, *Physical Review Letters* **119** (2017).
- [42] R. Moessner and S. L. Sondhi, *Equilibration and order in quantum Floquet matter*, *Nature Physics* **13**, 424 (2017).
- [43] V. Khemani, C. W. von Keyserlingk and S. L. Sondhi, *Defining time crystals via representation theory*, *Physical Review B* **96**, 115127 (2017).
- [44] W. W. Ho, S. Choi, M. D. Lukin and D. A. Abanin, *Critical Time Crystals in Dipolar Systems*, *Physical Review Letters* **119**, 010602 (2017).
- [45] J. Zhang, P. W. Hess, A. Kyprianidis, P. Becker, A. Lee, J. Smith, G. Pagano, I.-D. Potirniche, A. C. Potter, A. Vishwanath, N. Y. Yao and C. Monroe, *Observation of a discrete time crystal*, *Nature* **543**, 217 (2017).
- [46] S. Choi, J. Choi, R. Landig, G. Kucsko, H. Zhou, J. Isoya, F. Jelezko, S. Onoda, H. Sumiya, V. Khemani, C. von Keyserlingk, N. Y. Yao, E. Demler and M. D. Lukin, *Observation of discrete time-crystalline order in a disordered dipolar many-body system*, *Nature* **543**, 221 (2017).
- [47] J. Rovny, R. L. Blum and S. E. Barrett, *Observation of Discrete-Time-Crystal Signatures in an Ordered Dipolar Many-Body System*, *Physical Review Letters* **120**, 180603 (2018).
- [48] S. Pal, N. Nishad, T. S. Mahesh and G. J. Sreejith, *Temporal Order in Periodically Driven Spins in Star-Shaped Clusters*, *Phys. Rev. Lett.* **120**, 180602 (2018).
- [49] J. O’Sullivan, O. Lunt, C. W. Zollitsch, M. L. W. Thewalt, J. J. L. Morton and A. Pal, *Dissipative discrete time crystals* (2018).
- [50] A. Kyprianidis, F. Machado, W. Morong, P. Becker, K. S. Collins, D. V. Else, L. Feng, P. W. Hess, C. Nayak, G. Pagano, N. Y. Yao and C. Monroe, *Observation of a prethermal discrete time crystal*, *Science* **372**, 1192 (2021).
- [51] H. Taheri, A. B. Matsko, L. Maleki and K. Sacha, *All-optical dissipative discrete time crystals*, *Nature Communications* **13** (2022).
- [52] K. Sacha and J. Zakrzewski, *Time crystals: a review*, *Reports on Progress in Physics* **81**, 016401 (2018).
- [53] N. Yao, A. Potter, I.-D. Potirniche and A. Vishwanath, *Discrete Time Crystals: Rigidity, Criticality, and Realizations*, *Physical Review Letters* **118**, 030401 (2017).
- [54] A. Lazarides and R. Moessner, *Fate of a discrete time crystal in an open system*, *Phys. Rev. B* **95**, 195135 (2017).
- [55] F. Iemini, A. Russomanno, J. Keeling, M. Schirò, M. Dalmonte and R. Fazio, *Boundary Time Crystals*, *Physical Review Letters* **121**, 035301 (2018).
- [56] A. Lazarides, S. Roy, F. Piazza and R. Moessner, *Time crystallinity in dissipative Floquet systems*, *Phys. Rev. Res.* **2**, 022002 (2020).
- [57] K. Seibold, R. Rota and V. Savona, *Dissipative time crystal in an asymmetric nonlinear photonic dimer*, *Phys. Rev. A* **101**, 033839 (2020).
- [58] A. Riera-Campenya, M. Moreno-Cardoner and A. Sanpera, *Time crystallinity in open quantum systems*, *Quantum* **4**, 270 (2020).
- [59] M. Bauer, D. Bernard and A. Tilloy, *Computing the rates of measurement-induced quantum jumps*, *Journal of Physics A: Mathematical and Theoretical* **48**, 25FT02 (2015).
- [60] S. Luo and S. Fu, *Measurement-Induced Nonlocality*, *Phys. Rev. Lett.* **106**, 120401 (2011).
- [61] Z. Xi, X. Wang and Y. Li, *Measurement-induced nonlocality based on the relative entropy*, *Phys. Rev. A* **85**, 042325 (2012).
- [62] M.-L. Hu and H. Fan, *Dynamics of entropic measurement-induced nonlocality in structured reservoirs*, *Annals of Physics* **327**, 2343–2353 (2012).
- [63] M.-L. Hu and H. Fan, *Measurement-induced nonlocality based on the trace norm*, *New Journal of Physics* **17**, 033004 (2015).
- [64] B. Skinner, J. Ruhman and A. Nahum, *Measurement-Induced Phase Transitions in the Dynamics of Entanglement*, *Phys. Rev. X* **9**, 031009 (2019).
- [65] Q. Tang and W. Zhu, *Measurement-induced phase transition: A case study in the nonintegrable model by density-matrix renormalization group calculations*, *Phys. Rev. Res.* **2**, 013022 (2020).
- [66] S. Choi, Y. Bao, X.-L. Qi and E. Altman, *Quantum Error Correction in Scrambling Dynamics and Measurement-Induced Phase Transition*, *Phys. Rev. Lett.* **125**, 030505 (2020).
- [67] S.-K. Jian, C. Liu, X. Chen, B. Swingle and P. Zhang, *Measurement-Induced Phase Transition in the Monitored Sachdev-Ye-Kitaev Model*, *Phys. Rev. Lett.* **127**, 140601 (2021).
- [68] M. Buchhold, Y. Minoguchi, A. Altland and S. Diehl, *Effective Theory for the Measurement-Induced Phase Transition of Dirac Fermions*, *Phys. Rev. X* **11**, 041004 (2021).
- [69] T. Minato, K. Sugimoto, T. Kuwahara and K. Saito, *Fate of Measurement-Induced Phase Transition in Long-Range Interactions*, *Phys. Rev. Lett.* **128**, 010603 (2022).
- [70] Y. Li, Y. Zou, P. Glorioso, E. Altman and M. P. A. Fisher, *Cross Entropy Benchmark for Measurement-Induced Phase Transitions*, *Phys. Rev. Lett.* **130**, 220404 (2023).
- [71] P. Grelu and N. Akhmediev, *Dissipative solitons for mode-locked lasers*, *Nature Photonics* **6**, 84 (2012).
- [72] G. Schaller, in *Open Quantum Systems Far from Equilibrium* (Springer, Cham, 2014) pp. 1–26.
- [73] A. Altland and B. Simons, *Condensed matter field theory* (Cambridge University Press, Cambridge, England, 2006).
- [74] N. W. Ashcroft and N. D. Mermin, *Solid state physics* (Holt, Rinehart and Winston, 1976) p. 826.
- [75] B. Kramer and A. MacKinnon, *Localization: theory and experiment*, *Reports on Progress in Physics* **56**, 1469 (1993).
- [76] M. B. M. B. Priestley, *Spectral analysis and time series*, 3rd ed. (Academic Press, London, 1982).